UDK: 533.665:533.694.52
COSATI: 16-04, 20-04, 01-01

Analysis of the Rolling Moment Coefficients of a Rockets with Wraparound Fins

Slobodan Mandić, MSc (Eng)[1)]

The measurements of the rolling moment coefficients were done for two models with wraparound fins and one model with flat fins. The rolling moment coefficients were measured for two cant angles (0° and 0.8°). The measured values were fitted by the fourth order polinom of the angle of attack. It was proven that the rolling moment coefficient at zero angle of attack is equal to the sum of the rolling moment coefficient due to the curvature of the fins and rolling moment coefficient of the canted equivalent flat fins.

Key words: **missile aerodynamics, wraparound fins, rolling moment, aerodynamic coefficients, derivatives of the aerodynamic coefficients.**

Notation and symbols

$Oxyz$ – Body axis system
$Oxy'z'$ – Semi-fixed, non-rolling axis system
$Ox\bar{y}\bar{z}$ – Aerodynamic axis system
C_ℓ – Rolling moment coefficient
G_0 – Zero term of Fourier's series
H_4 – Amplitude of the sine harmonics of Fourier's series
ϕ – Model roll angle
ϕ_α – Aerodynamic roll angle
ϕ_α^* – Angle of orientation of the plane of the total angle of attack with respect to the vertical plane
α – Angle of attack
α_e – Angle of attack in the wind tunnel
C_{ℓ_0} – Rolling moment coefficient at $\alpha = 0$ zero angle of attack
$C_{\ell\alpha^2}$ – Derivative of the rolling moment coefficient due to α^2
$C_{\ell\alpha^4}$ – Derivative of the rolling moment coefficient due to α^4
$C_{\ell_{00}}$ – Rolling moment coefficient due to curvature of the wraparound fins
$C_{\ell_{\delta_\ell}}$ – Derivative of the rolling moment coefficient due to cant angle of the fins

Introduction

THE predominant reason for the design of a tube launcher of the missile is packaging convenience. The tube launcher requires folding wraparound fins (WAF) which are deployed instantlly after the missile has left the tube of the launcher [1].

Some of the characteristics of a missiles with wraparound fins are different comparing to the missiles with flat fins and it has been investigated for years [1], [2], [14].

It was shown by exeperiments that the static longitudinal characteristics of the missile with wraparound fins did not differ from the static longitudinal characteristics of the missile with flat fins with the area equal to the projected area of the curved fins [2]. It was also proven that there is no increase of the total drag.

It was determined by the experimental data from the various wind tunnels that wraparound fins develop the rolling moment even at zero angle of attack and zero cant angle of the fins. This moment has the direction towards the centre of the curvature of the fins at subsonic speeds and changes the direction at supersonic speeds. This rolling moment is called induced rolling moment [2].

A possible reason for the induced rolling moments in subsonic flight of the missile with WAF is found in the converging separated wake generated at the base of the configuration [2]. According to the assumption that the base flow is responsible for the induced rolling moment, it was shown by theoretical investigation that moving the fins upstream should reduce this moment. It is also stated that forward sweep of the trailing edge sharply reduces the rolling moment. The experimental data was given for only two Mach numbers $M = 0.5$ and $M = 0.8$.

The reduction of the rolling moment with the increase of the Mach number was investigated in [3]. It was shown by experimental investigation for Mach number $M = 2.15 \div 3.83$ that the rolling moment decreased rapidly by a factor nearly 2 between Mach numbers of 2.15 and 2.41.

The influence of the fin leading and trailing edges on the rolling moment coefficients for the missile Mk66 is given in [4]. The diagrams for the rolling moment coefficient are given as a function of the Mach numbers for a different type of leading and trailing edges and the standard fins

1) Military Technical Institute (VTI), Ratka Resanovića 1, 11132 Belgrade

canted for the angle 1.5 degrees

Comparison of the rolling moment coefficients computed by the full Naviar-Stokes code and coefficients obtained experimentally was done in [5]. The computed rolling moment coefficients for velocities ranging from Mach 1.3 to Mach 3.0 showed favourable agreement with experimental data. The calculated and experimental data showed that the crossover point is greater than Mach 1.0. The results of CFD computations do not indicate that the rolling moment coefficient is Reynolds number dependent.

A wall mounted semi-cylindrical model fitted with a single wraparound fin was investigated both numerically and experimentally for Mach numbers 2.8-4.9 [12]. The rolling moment rapidly decreased (almost discontinuously) by factor of nearly 2 between Mach numbers of 2.28 and 2.41. For $M \geq 2.41$ the rolling moment decreased almost linearly with the increasing of the Mach number. The slotted fin also displayed a trend of decreasing the rolling moment with the Mach number. The magnitude of the rolling moment of the slotted fin is twice the one of the solid fin.

In order to avoid aerodynamic anomalies of the wrap-around fins the alternative configurations were investigated in [13]. One alternative to wraparound fins is FLEX fins which deploy straight fins to some offset angles less than perpendicular. Another improvement to wrap-around fins is the use of slots. It was shown that the slots reduce the out of plane moment and decrease the roll rate dependence with Mach number.

The rolling moment coefficient vs. the angle of attack for the solid and slotted fin configurations was compared for Mach numbers from 0.5 to 3.0 in [14]. Dependance of the C_ℓ vs. the angle of attack is of parabolic nature. Rolling momnet coefficient increases negatively as the angle of attack increases. All C_ℓ data for the slotted fins have shifted upwords positively compared to the solid fins. At high Mach numbers $(M > 1.5)$ C_{ℓ_0} is negative for both the solid and slotted fin. At Mach number 1.5 the solid fins have a negative C_{ℓ_0} while the slotted fins have positive C_{ℓ_0}. All the subsonic C_{ℓ_0} data for the slotted fins is negative while it is positive for the solid fins.

The purpose of this paper is to investigate the influence of the canted wraparound fins on the rolling moment coefficients relative to the canted equivalent flat fins. Since the cant angle of the fins of the unguided missiles are small $\left(\leq 2^\circ\right)$ the initial assumption is that the rolling moment of the missile with canted wraparound fins is equal to the sum of the rolling moment of the missile with equivalent flat fins and rolling moment of the wraparround fins with zero cant angle.

Rolling moment coefficient

The most convenient way to analyze the rolling moment coefficient is to study it in terms of the parameters in aerodynamic axis system $O\overline{xyz}$ (axys system related to the total angle of attack) [14, 15]. The $O\overline{x}$ axis is connected to the longitudinal axis of the missile and directed to the tip of the missile, $O\overline{z}$ is in the plane of total angle of attack and $O\overline{y}$ is normal to the incidence plane (Fig.1). The plane of total angle of attack (incidence plane) is a plane containing velocity vector and missile longitudinal axis.

Angle of orientation of the plane of the total angle of attack ϕ_α relative to the body axis system $Oxyz$ is defined ny the following formula:

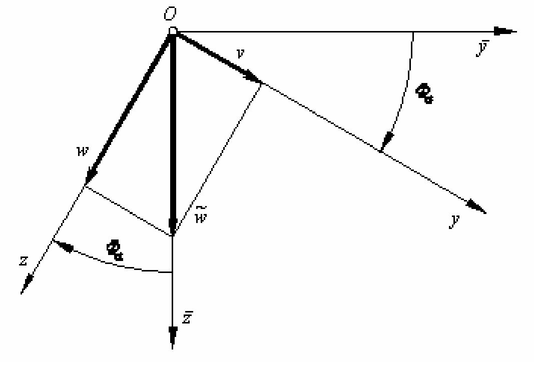

Figure 1. Relations between body and aerodynamic axis

$$\phi_\alpha = \arctan\frac{v}{w} \tag{1}$$

where v and w are lateral speeds in the body axis system.

Rolling moment coefficient for unguided missile in aerodynamic axis system can be written in the following form [15], [16].

$$\overline{C}_\ell = G_0 + H_4 \sin 4\phi_\alpha \tag{2}$$

where

$$\begin{aligned} G_0 &= C_{\ell_0} + C_{\ell_{\alpha^2}}\alpha^2 + C_{\ell_{\alpha^4}}\alpha^4 \\ H_4 &= C^{(4)}_{\ell_{\alpha^4}}\alpha^4 \end{aligned} \tag{3}$$

Semifixed axis system (non-rolling axis system) $Ox'y'z'$ is frequently used for wind tunnel data presentation. The Ox' axis coincides with longitudinal axis of the missile, Oz' axis is pointed vertically down and Oy' is normal to the Oz' axis. The roll angle of the model ϕ is the angle between $Ox'y'$ plane of semi-fixed axis system and Oxy plane of body axis system (Fig.2).

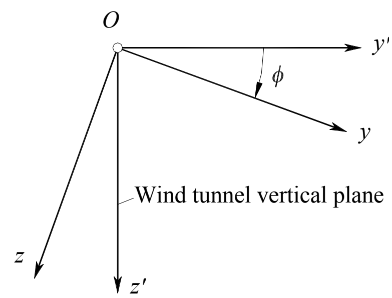

Figure 2. Relations between semi-fixed and body axis.

In the wind tunnel test the angle between the model and the air strem (angle of attack) is changed from negative to positive values. The roll angle of the model around the longitudinal axis relative to the semifixed axis system is constant for one run.

The orientation angle of the plane of the total angle of attack relative to semifixed (nonrotating) axis system has two values:

$$\phi_\alpha^* = 0^\circ \text{ for } \alpha_e \geq 0$$
$$\phi_\alpha^* = 180^\circ \text{ for } \alpha_e < 0 \tag{4}$$

Substituting the relation between angles ϕ_α and ϕ

$$\phi_\alpha = \phi - \phi_\alpha^* \tag{5}$$

in equation (2) the rolling moment coefficient can be written as a function of angle ϕ which is constant for one run.

$$\overline{C}_\ell = G_0 + H_4 \sin 4\phi \tag{6}$$

Description of the model

The basic dimensions of the model are given in Fig.3.

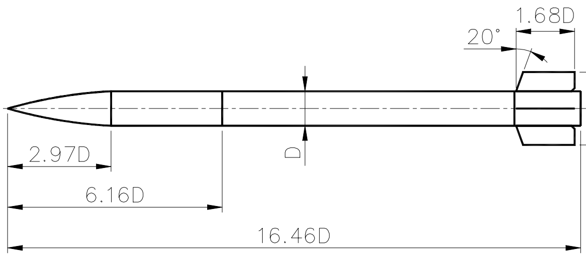

Figure 3. The basic dimensions of the model

There are three configurations of the model. The body of the missile with ogival nose is the same for all three models. The wing sections of the model are changed in order to cbtain different models. Two wing sections have wrap-around fins and the third section has equivalent flat fins. The wraparound fins have the same dimensions, but one set of the fins has the opposite curvature to the other. The flat fins are obtained by projection of the wraparound fins on the plane which goes through the longitudinal axes of the missile and root cord of the wraparound fins. The rear view of the three configurations of the model is given in Fig. 4. These three configurations are designated as *Model-1*, *Model-2* and *Model-3.*

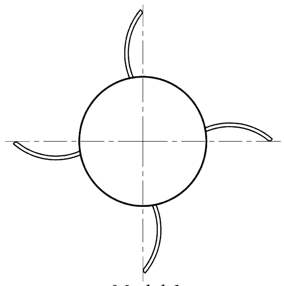

Model 1

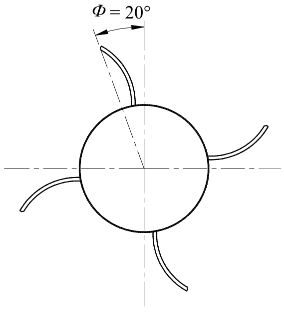

Model 2

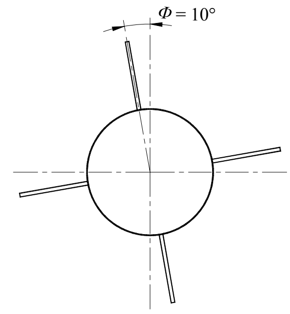

Model-3

Figure 4. Rear view of the fins section

The plane which goes through the longitudinal axes of the missile and root cord of the wraparound fins was rotated for an angle $\phi = 10^o$ relative to the vertical plane. *Model 2* has the wraparround fins with opposite curvature to the fins of the *Model 1.* The plane which connects the tips of the fins was rotated for a roll angle $\phi = 20^o$ relative to the vertical plane of the wind tunnel (incidence plane).

In order to find the relation between the rolling moment coefficient of the missile with wraparound fins and rolling moment coefficient of the missile with flat fins, the measurements of the rolling moment coefficient were done for two cant angles $\delta_\ell = 0.0^o$ and $\delta_\ell = 0.8^o$ (Fig.5).

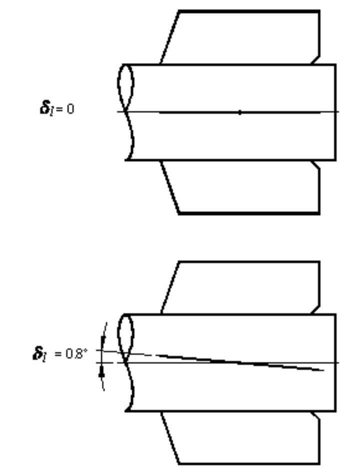

Figure 5. Cant angle of the fins

Measurement results

The measured data of the rolling moment coefficients for all three models are given in Figures 6 – 11. Since the rolling moment coefficients of the wraparound fins at zero angle of attack have different sign in subsonic region from the sign in supersonic region, the graphical representations of the measurements are chosen for Mach numbers $M = 0.7$ and $M = 2.0$. There are two curves on each of the diagrams, one for zero cant angle of the fins $\left(\delta_\ell = 0^\circ\right)$ and the other for $\delta_\ell = 0.8^o$.

In order to determine $C_{\ell_{\alpha^4}}$ and $C_{\ell_{\alpha^4}}^{(4)}$ it is necessary to have at least two runs: for the roll angle $\phi = 0^o$ and roll angle $\phi = 22.5^o$. There are measurements available only for one roll angle for each of the models (*Model 1*- $\phi = 0^o$, *Model 2* - $\phi = 20^o$ and *Model 3* - $\phi = 10^o$), so it is impossible to distinguish the derivative $C_{\ell_{\alpha^4}}$ from the derivative $C^{(4)}_{\ell_{\alpha^4}}$.

Since the purpose of this paper is to determine the contribution of the curvature of the wraparound fins to the rolling moment coefficient, fitting of the experimental data will be done by the fourth order polinom without distinction between derivatives $C_{\ell_{\alpha^4}}$ and $C^{(4)}_{\ell_{\alpha^4}}$.

The rolling moment coefficient can be written in the polinominial form as even function of the angle of attack.

$$C_\ell = C'_{\ell_0} + C_{\ell_{\alpha^2}}\alpha^2 + C_{\ell_{\alpha^4}}\alpha^4 \qquad (7)$$

The fitted curves are given on the same diagrams with experimental data and analysis of the results of the fitting will be given seperatelly for each of the models.

Model 1

Results of the measurements of the rolling moment coefficients for *Model 1* are given in Fig.6 for $M = 0.7$ and Fig.7 for $M = 2.0$. The derivatives of the rolling moment coefficient (7) obtained by fitting experimental data for all the investigated Mach numbers are given in Table 1 and Table 2 ($\delta_\ell = 0^o$ and $\delta_\ell = 0.8^o$).

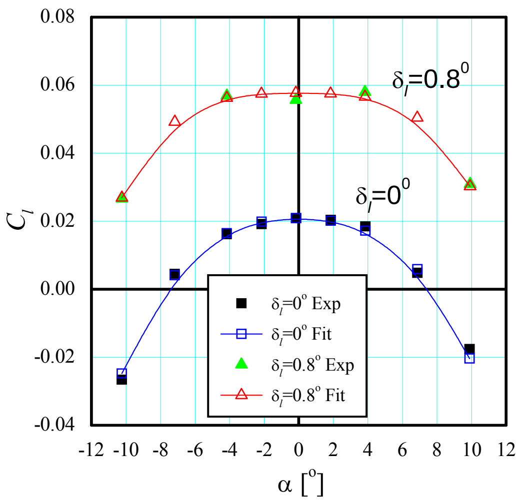

Figure 6. C_ℓ for *Model 1* - $M = 0.7$

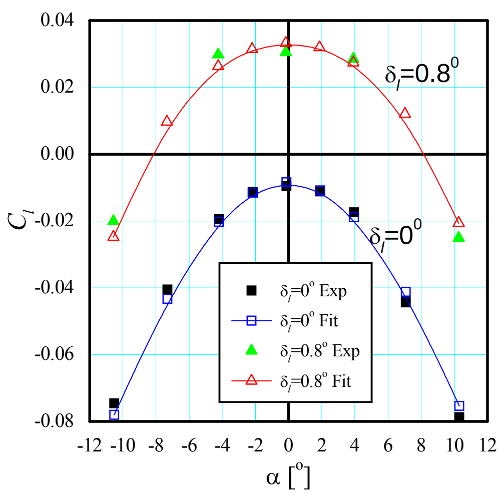

Figure 7. C_ℓ for *Model 1* - $M = 2.0$

Table 1 Derivatives of the rolling moment coefficient for $\delta_\ell = 0^o$: *Model 1*

M	0.5	0.7	0.9	1.0	1.1	1.5	2.0
C_{ℓ_0}	0.0208	0.0209	0.0214	0.0144	0.0111	0.0048	-0.0084
$C_{\ell_{\alpha^2}}$	-0.394	-0.722	-1.215	-1.97	-2.725	-0.952	-2.233
$C_{\ell_{\alpha^4}}$	-44.2	-22.3	-0.62	25.1	68.3	-8.62	4.96

Table 2 Derivatives of the rolling moment coefficient for δ_ℓ=0.8^o : *Model 1*

M	0.5	0.7	0.9	1.0	1.1	1.5	2.0
C_{ℓ_0}	0.0582	0.0577	0.0553	0.0527	0.044	0.0221	0.0332
$C_{\ell_{\alpha^2}}$	-0.131	-0.131	0.164	-0.624	-0.525	0.394	-1.182
$C_{\ell_{\alpha^4}}$	-44.19	-26.2	-17.8	1.33	-6.06	-31.4	-15.5

Model 2

Rolling moment coefficients for *Model 2* increase with the increase of the angle of attack (Fig.8 for $M = 0.7$ and Fig.9 for $M = 2.0$). It is particularly evident in case when the fins are canted for an angle $\delta_\ell = 0.8^o$. The derivatives of the rolling moment coefficient for all the investigated Mach numbers, obtained by fitting experimental data, are given in Table 3 for $\delta_\ell = 0^o$ and Table 4 for $\delta_\ell = 0.8^o$.

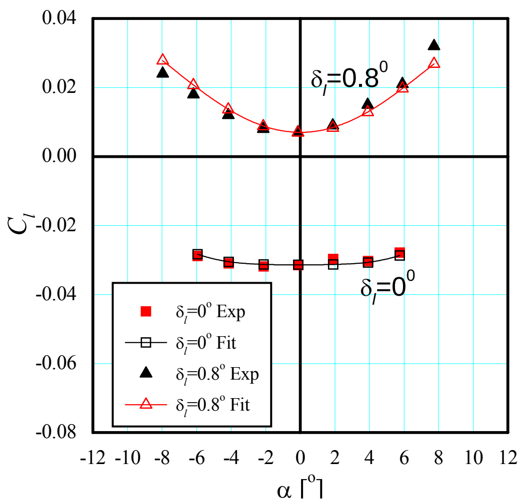

Figure 8. C_ℓ for *Model 2* - $M = 0.7$

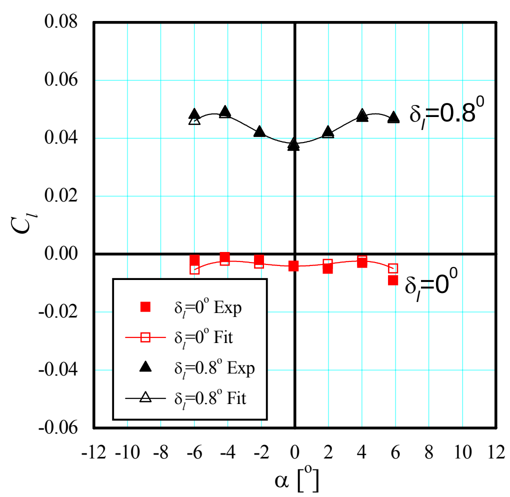

Figure 9. C_ℓ for *Model 2* - $M = 2.0$

Table 3 Derivatives of the rolling moment coefficient for $\delta_\ell = 0^\circ$: *Model 2*

M	0.5	0.7	1.75	2.0
C_{ℓ_0}	-0.0326	-0.0313	-0.0115	-0.0042
$C_{\ell_{\alpha^2}}$	0.46	0.0253	1.94	0.82
$C_{\ell_{\alpha^4}}$	-47.0	23.72	-107.8	-84.8

Table 4 Derivatives of the rolling moment coefficient for δ_ℓ=0.8° : *Model 2*

M	0.5	0.7	0.9	1.0	1.1	1.5	2.0
C_{ℓ_0}	0.0049	0.0069	0.006	0.0108	0.0165	0.0184	0.0379
$C_{\ell_{\alpha^2}}$	1.083	1.346	2.988	3.086	2.63	5.089	3.086
$C_{\ell_{\alpha^4}}$	-21.11	-13.64	-107.8	-107.8	-75.67	-215.3	-215.7

Table 5 Derivatives of the rolling moment coefficient for $\delta_\ell = 0^\circ$: *Model 3*

M	0.5	0.7	0.9	1.0	1.75	2.0
C_{ℓ_0}	-0.0001	-0.0006	0.0013	-0.0013	-0.0002	-0.0011
$C_{\ell_{\alpha^2}}$	1.149	1.15	0.525	-0.295	1.149	0.689
$C_{\ell_{\alpha^4}}$	-106.6	-101.1	-58.75	10.97	-215.6	-107.8

Table 6 Derivatives of the rolling moment coefficient for δ_ℓ=0.8° : *Model 3*

M	0.5	0.7	0.9	1.0	1.5	2.0
C_{ℓ_0}	0.0324	0.0344	0.0336	0.0325	0.0219	0.0357
$C_{\ell_{\alpha^2}}$	2.922	2.43	2.594	2.856	4.465	2.594
$C_{\ell_{\alpha^4}}$	-215.6	-107.6	-107.8	-109	-215.6	-216

Model 3

Dependence of the rolling moment coefficients on the angle of attack for the *Model 3* ,is similar to the *Model 2* (Fig.10 for $M = 0.7$ and Fig.11 for $M = 2.0$). The rolling moment coefficients are close to zero when the fins are not canted. Derivatives of the rolling moment coefficient for all the investigated Mach numbers for the Model-3 are given in Table 5 $\left(\delta_\ell = 0^\circ\right)$ and Table 6 $\left(\delta_\ell = 0.8^\circ\right)$.

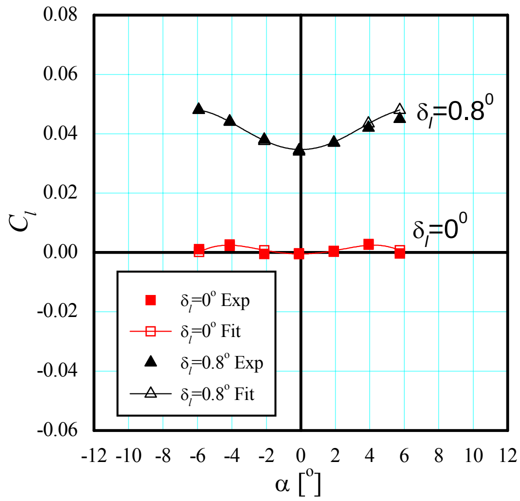

Figure 10. C_ℓ for *Model 3* - $M = 0.7$

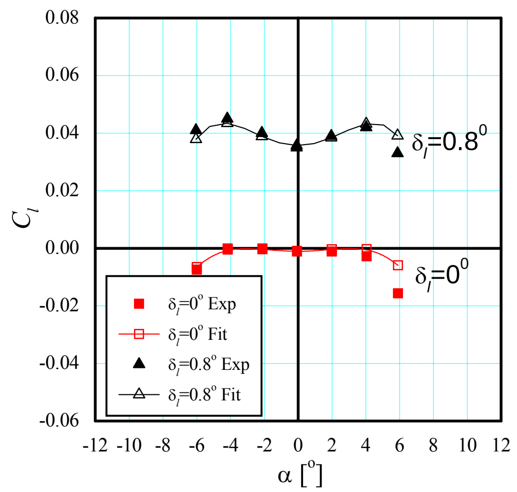

Figure 11. C_ℓ for *Model 3* - $M = 2.0$

Rolling moment due to the curvature of the fins

The rolling moment coefficients at zero angle of attack $\left(C_{\ell_0}\right)$ in function of the Mach number are given in Figures 12 - 14 for *Model 1*, *Mode 2* and *Model 3* respectively.

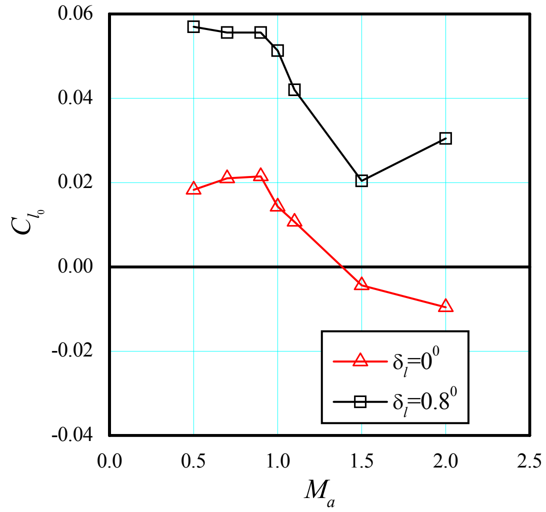

Figure 12. *Mode 1:* C_{ℓ_0} for $\delta_\ell = 0^\circ$ and $\delta_\ell = 0.8^\circ$

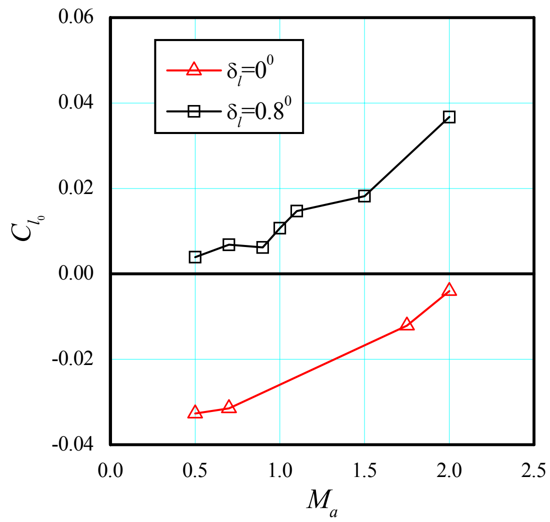

Figure 13. *Model 2:* C_{ℓ_0} for $\delta_\ell = 0^\circ$ and $\delta_\ell = 0.8^\circ$

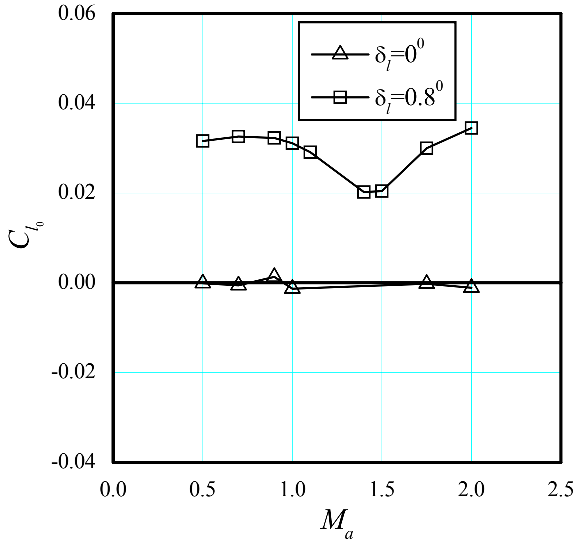

Figure 14. *Model 3:* C_{ℓ_0} for $\delta_\ell = 0.8^\circ$

There are two curves on each of the diagrams: one curve is for zaro cant angle and the other is for fins canted for an angle $\delta_\ell = 0.8^\circ$.

The rolling moment coefficients due to the curvature of the fins are obtained by substituting the rolling moment coefficients of the missile with flat fins from the appropriate rolling moment coefficients of the missile with wraparound fins (ΔC_{ℓ_0}). As the result of the substraction, the rolling moment coefficients due to the curvature of the wraparound fins are obtained as a function of the Mach number.

Since the curvature of the wraparound fins for the *Model 1* equal to the curvature of the wraparound fins for *Model 2* the rolling moment coefficients for zero cant angle must be equal but with opposite signs. The rolling moment coefficients obtained by both the measurement of the models with zero cant angle of the wraparound fins and the difference of rolling moment coefficients of the models with wraparound fins and model with flat fins are given in Fig.15 as a function of the Mach number.

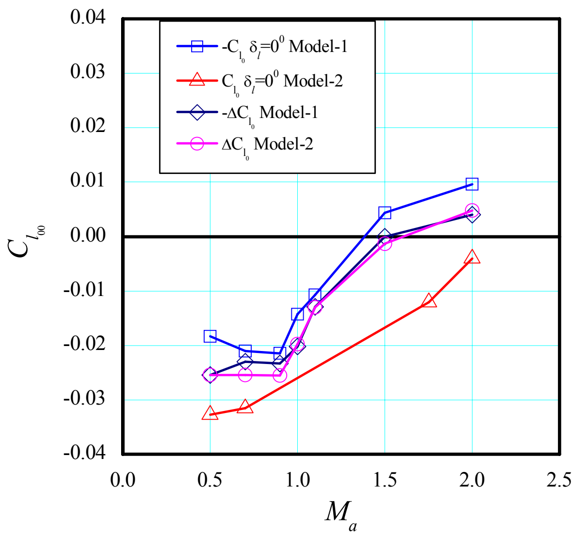

Figure 15. $C_{\ell 0}$ as a function of the Mach numbers

The curves which represent the contribution of the wraparound fins curvature to the rolling moment coefficient of the model with flat fins $(\Delta C_{\ell 0})$ have good agreement with the rolling moment coefficients for the zero canted fins of the *Model 1*. This statement is not valid for *Model 2*. There is no physical exlanation for the deviation of the zero rolling moment coefficients of the *Model 2* from the zero rolling moment coefficients of the *Model 1* and increament $\Delta C_{\ell 0}$ for both models.

It can be concluded from the diagrams in Figures 12 - 14, that the rolling moment coefficient of the missile with wraparound fins can be written as the sum of the moment due to the curvature of the fins and the moment due to the cant angle of the fins.

$$C_{\ell_0} = C_{\ell_{00}} + C_{\ell_{\delta_\ell}} \delta_\ell \qquad (3)$$

The zero term $C_{\ell_{00}}$ is shown in Fig.15.

The derivative $C_{\ell_{\delta_\ell}}$ can be calculated from the measurements of the rolling moment coefficients of the missile with canted flat fins. The diagram of the derivative $C_{\ell_{\delta_\ell}}$ as a function of the Mach numbers is given in Fig16.

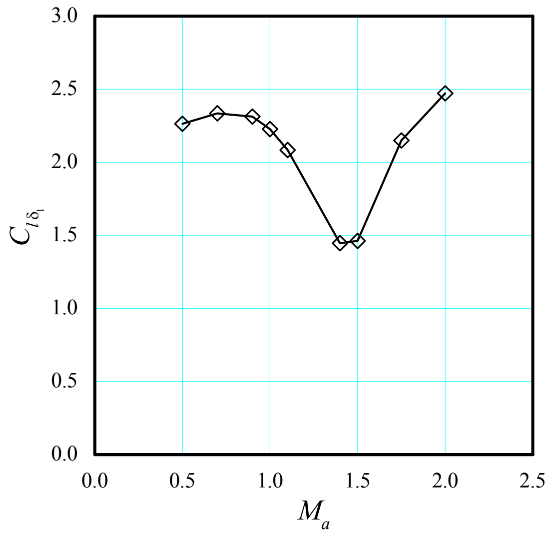

Figure 16. Derivative $C_{\ell_{\delta_\ell}}$

Conclusion

Measurement of the rolling moment coefficients is done for three models. Two models are with wraparound fins and one model is with flat fins. The flat fins are obtained by projection of the wraparound fins on the plane through longitudinal axis and root chord of the wraparound fins.

It is proven by the measurements of the rolling moment coefficient that the rolling moment coefficient is an even function of the angle of attack.

The rolling moment coefficient is expressed in the form of Fourier's series in the aerodynamic axis system. Hence, there are no measured data for the roll angle $\phi = 22.5^\circ$, it is impossible to separate coefficient $C^{(4)}_{\ell_{\alpha^4}}$ of the fourth order term from the coefficient $C_{\ell_{\alpha^4}}$ of the zero term of the Fourier's series.

The measured rolling moments are fitted by the polinom of the fourth order and as the results of the fourth order and as the results of the fitting the coefficients C_{ℓ_0}, $C_{\ell_{\alpha^2}}$ and

$C_{\ell_{\alpha^4}}$ are obtained for all.

It is also shown that the rolling moment coefficient at zero angle of attack is equal to the sum of the rolling moment coefficients due to the curvature of the fins and rolling moment coefficient of the canted equivalent flat fins.

References

[1] Design of aerodynamically stabilized free rockets – Military Handbook MIL-HDBK-762 (MI) 17 July 1990.

[2] BAR-HAIM,B., SEGINER,A.: *Aerodynamics of Wraparound Fins*, J. Spacecraft, July-August 1983, Vol.20, No 4.

[3] MCINTYRE,T.C., BOWERSOX,R.D.W., GOSS,L.P.: *Effects of Mach Number on Supersonic Wraparound Fin Aerodynamics*, Nov/Dec 1998, Vol.35, No.6, pp.742-748.

[4] Bergbauer,D.M., FERGUSON,J.H., BEWRGMAN,R.W., BENTLEY,R.: *Spin Profile Tailoring for the Improved 2.75-inch Rocket*, AIAA Paper No.80-1575.

[5] EDGE,H.L.: *Computation of the Roll Moment for a Projectile with Wrap_Around Fins*, Journal of Spacecraft and Rockets, July-August 1994, Vol.31, No.4.

[6] WINCHENBACH,G.L., BUFF,R.S., WHYTE,R.H., HATHAWAY,W.H.: *Subsonic and Transonic Aerodynamic of a Wraparound Fin Configuration*, Journal of Guidance, Control, and Dynamics, 1986, Vol.9, No.6, pp.627-632.

[7] MIKHAI,A.G.l: *Roll damping for projectiles including wraparound*, offset, and arbitrary number of fins, Journal of Spacecraft and Rockets, Nov/Dec 1995, Vol.32,. pp.929-37.

[8] CATANI,U., BERTIN,J.J., BOUSLOG,S.A.: *Aerodynamics Characteristics for a Slender Missile with Wrap-Around Fins*, Journal of Spacecraft and Rockets, March-April 1983, Vol.20, No.2, pp.122-128.

[9] SAWYER,W.C., MONTA,W.J., CARTER,W.V.,: *Control characteristics for Wrap-Around fins on cruise Missile Configuration*, J.Spacecraft, March-April 1982, Vol.19, No.2,.pp.150-154.

[10] TILMANN,C.P., HUFFMAN,R.E., JR.BUTER,T.A., BOWERSOX,R.D.W.: *Experimental Investigation of the Flow structure near a Single Wraparound Fin*, Journal of Spacecraft and Rockets, 1997, Vol.34, No.6, pp.729-736.

[11] LUCERO,E.F.: *Subsonic Stability and Control Characteristics of Configurations Incorporating Wrap-Around Surfaces,* Journal of Spacecraft and Rockets, 1976, Vol.13, No.12, pp.740-745.

[12] TILMANN,C.P., MCINTYRE,T.C., BOWERSOX,R.D.W., BUTER,T.A.: *Aerodynamic of Wrap-Around Fins at High Supersonic Speeds*, RTO AVT Symposium on Missile Aerodynamics, Sorrento, Italy, 11-14 May 1998.

[13] ABATE,G.L., WINCHENBACH,G.: *Analysis of Wrap-Around Fin and Alternative Deployable Fin System for Missiles*, Meetings "Subsystem Integration for Tactical Missiles (SITAM) and Design and Operation of Unmanned Air Veicles (DOUAV)", Ankara, Turkey, 1995.

[14] BERNER,C., ABATE,G., DUPUIS,A.: *Aerodynamics of Wrap Around Fins using Experimental and Computational Techniques*, RTO AVT Symposium on Missile Aerodynamics, Sorrento, Italy, 1998.

[15] ĆUK,D., ĆURČIN,M., MANDIĆ,S.: *The Method of the Determination of the Nonlinear Aerodynamic Coefficients in Descartes Coordinates Depending on the Different Types of Missile Symmetry from Static Wind-Tunnel Test Data – The Program Fitalpha – theoretical manual*, Belgrade, MTI, 2001.

[16] ĆUK,D., ĆURČIN,M., MANDIĆ,S.: *The Method of the Determination of the Nonlinear Missile Aerodynamic Coefficients in the Polar Form from Static Wind-Tunnel Test Data – The Program Fitphi – theoretical manual*, Belgrade, MTI, 2001.

Received: 28.06.2006.

Analiza koeficijenta momenta valjanja raketa sa olučastim krilima

Merenje koeficijenta momenta valjanja u aerotunelu, urađeno je za dva modela raketa sa olučastim krilima i jedan model rakete sa ravnim krilima. Merenje koeficijenta momenta valjanja za sve modele urađeno je za dva ugla ugradnje krila (0° i 0.8°). Izmerene vrdnosti koeficijenta momenta valjanja usklađene su sa polinomom četvrtog stepena po napadnom uglu. Pokazano je da je koeficijent momenta valjanja raketa sa olučastim krilima, pri nultom napadnom uglu, jednak zbiru koeficijenta momenta valjanja usled krivine olučastih krila i koeficijenta momenta valjanja ekvivalentnih ravnih krila postavljenih pod istim uglom ugradnje kao i olučasta krila.

Ključne reči: **arodinamika rakete, olučasto krilo, momenta valjanja, aerodinamički koeficijenti, aerodinamički derivativi.**

Анализ коэффициента момента вращения ракет со нарезными килями

Измерение коэффициента момента вращения в аэродинамической трубе проведено для двух моделей ракет со нарезными килями и для одной модели ракеты с гладкими (ровными) килями. Измерение коэффициента момента вращения для всех моделей проведено для двух углов установки киля (0° и $0{,}8^{\circ}$). Измеренные величины коэффициента момента вращения согласованы с многочленом четвёртой ступени угла атаки. Здесь показано, что коэффициент момента вращения ракет со нарезными килями, при нулевом угле атаки, одинаков сумме коэффициента момента вращения из-за кривой нарезных килей и коэффициента момента вращения эквивалентных гладких (ровных) килей, установленных под таким же углом установки, под каким и нарезные кили.

Ключевые слова: аэродинамика ракеты, нарезной киль, момент вращения, аэродинамические коэффициенты, аэродинамические деривативы.

Analyse des coefficients du moment de roulement chez les missiles aux ailes enveloppées

Le mesurement des coefficients du moments de roulement a été réalisée dans la soufflerie pour deux modèles des missiles aux ailes enveloppées et pour un modèle aux ailes plates. Pour tous les modèles on a fait le mesurement du coefficient du moment de roulement pour deux angles de pose des ailes (0° et 0.8°). Les valeurs mesurées du coefficient du moment de roulement sont accordées avec le polynôme à la quatrième puissance quant à l'angle d'attaque. On a démontré que le coefficient du moment de roulement des missiles aux ailes enveloppées, à l'angle d'attaque zéro, est égal à la somme des coefficients du moment de roulement à cause de la courbature des ailes enveloppées et des coefficients du moment de roulement des ailes plates équivalentes posées sous la même angle que chez les ailes enveloppées.

Mots clés: **aérodynamique du missile, aile enveloppée, moment de roulement, coefficients aérodynamiques, dérivatifs aérodynamiques.**